K-shell processes in heavy-ion collisions in solids and the local plasma approximation

Umesh Kadhane,[1] C. C. Montanari,[2] and Lokesh C. Tribedi[1]
[1]*Tata Institute of Fundamental Research, Homi Bhabha Road, Colaba, Mumbai 400 005, India*
[2]*Instituto de Astronomía y Físca del Espacio, CONICET-UBA, Buenos Aires, Argentina*
(Received 19 July 2002; published 12 March 2003)

We have investigated *K*-shell vacancy production due to ionization and electron transfer processes, in collisions of highly charged oxygen ions with various solid targets such as Cl, K, Ti, Fe, and Cu at energies between 1.5 and 6.0 MeV/u. The *K*-shell ionization cross sections were derived from the measured *K* x-ray cross sections. An *ab initio* theoretical model based on the local plasma approximation (LPA), which is an extension of the dielectric formalism to consider core electrons, provides an explanation of the measured data only qualitatively. In case of asymmetric collisions ($Z_p/Z_t<0.35$, Z_p, Z_t being the atomic numbers of the projectile and target, respectively) and at higher energies, the LPA model explains the data to some extent but deviates for more symmetric collision systems. On the other hand, a perturbed-stationary-state (PSS) calculation (ECPSSR), including the corrective terms due to energy (*E*) loss, Coulomb (*C*) deflection, and relativistic (*R*) wave functions designed for ion-atom collisions agree quite well with the data for different combinations of target and projectile elements. In addition, we have also measured the *K*(target)-*K*(projectile) electron transfer cross sections and compared them with a model based on perturbed-stationary-state approximation.

DOI: 10.1103/PhysRevA.67.032703 PACS number(s): 34.50.Fa, 34.70.+e, 34.50.Bw

I. INTRODUCTION

The study of heavy-ion induced inelastic processes involving strongly bound electrons in the inner shells of atoms remains interesting in spite of a large number of experimental and theoretical investigations. It is well known that when the projectile velocity v_p is approximately equal to the electron orbital velocity v_e, various processes such as ionization, electron capture and excitation have maximum cross sections and are of the same order of magnitude. Ionization and electron transfer involving inner shells are the two dominant processes in case of heavy-ion collisions. There have been numerous studies on the total ionization cross sections of the deeply bound electrons and several empirical scaling laws [1,2] have been proposed. For beam energies of a few MeV/u, the so-called velocity matching condition is satisfied for the deeply bound electrons of low atomic number target elements and therefore the cross sections for the inner-shell electron transfer and ionization reach their maxima. The projectile velocities are too large for the outer or loosely bound electrons, making the cross sections for those processes very small ($\sim v_p^{-11}$). There are many measurements on the total electron-capture cross sections for initially loosely bound electrons and several empirical scaling laws [3,4] have been proposed to calculate the cross sections of such a process. But, the state selective electron transfer cross sections involving deeply bound initial and final states cannot be described by such simple empirical laws and the mechanisms of such transfer processes are not yet understood completely.

The present collision systems are highly nonperturbative, since the initial states (as well as final states) are highly distorted by the long-range Coulomb interaction with the highly charged ions. Therefore, the first-order Born approximation ($B1$) fails to calculate the total cross sections for the inner-shell ionization as well as transfer. In order to include the effect of distortion of the initial-state wave function as well as polarization by the heavy-ion impact, in one approach, Brandt and co-workers [1,5,6] developed a model which is commonly known as ECPSSR and is generally used to calculate the inner-shell ionization cross sections. This model is based on perturbed stationary-state (PSS) approximation with modifications due to enhanced binding energy, Coulomb (C) deflection, energy loss (E), and relativistic (R) effects, introduced in the $B1$ calculations in a semiempirical manner. It has become a convention to compare the experimental results with this theory, since it provides an analytical expression for inner-shell ionization and also for its universal scaling rule. Similar calculations have been developed to describe the electron capture from an inner shell (see below). However, it may be mentioned that these PSS calculations are not *ab initio*.

On the other hand, we present here an alternative model to describe the interaction of the swift ions with the inner-shell electrons of the solids. The usual formalism to deal with collisions involving solid targets is the dielectric theory, first proposed by Bohr [7] and extensively employed since then [8]. Within this formalism, the target electrons are considered to respond collectively to the passage of the projectile. The polarization of the medium can be described as a wake of density fluctuation trailing the ion, producing a wake-induced electric field. This response of the electrons in the solid to the ion perturbation is known as the solid-state effect [9–15].

It may be difficult to provide a quantitative estimation of the contribution in the inner-shell ionization cross section arising due to the solid-state effect. However, previous measurements have shown that the solid-state effect could enhance the radiative electron-capture process by about 50% [11] or more compared to that for gas targets. One has also observed an enhancement of about 15–20 % of the projectile Lyman-α x-ray intensity (following electron capture) in ion-solid [12] and in ion-fullerene [13,14] collisions, over that

for ion-atom collisions. However, these enhancements depend on Z_p and v_p.

The experiments at high velocities ($v_p \sim 36$ a.u.) have also shown that the target inner-shell electrons must be taken into account to have a complete picture of the dynamical screening of the ion [15–17]. One of the models to deal with core electron polarization is the local plasma approximation (LPA) [17–20]. It describes bound electrons as a free-electron gas of inhomogeneous density, and uses a spatial mean value of the dielectric response of these electrons. There have been many applications of this model, from the original proposal of Lindhard and co-workers [18] to more recent calculations of coupling of projectile orbitals by the induced potential [17] or the contribution of deep bound electrons to the stopping power and energy straggling [20,21] providing results in good accord with the experimental measurements.

Though the LPA has been formulated to describe the core-electron response as a whole, the present version incorporates the description of shell to shell response. In this way, it allows us to consider the excitation of each shell separately, for instance to evaluate *K*-shell ionization. The employment of the LPA in this case means exploring the borders of validity of the model.

The LPA has been shown to be valid in the high-energy regime [17,20,21]. This work is an attempt to test the validity of the LPA to deal with inner-shell ionizaton in the intermediate velocity range ($v_p \sim 6-14$ a.u., $v_p/v_e \sim 0.3-1.1$). Since the applicability of the theoretical models depends on the symmetry parameter ($S_Z = Z_p/Z_t$) and hence on the perturbation strength of the collision, we have chosen a set of low Z_t targets in order to have a variation of S_Z over a wide range (between 0.27 and 0.48).

II. THE THEORETICAL MODEL: LPA

As described above, the LPA [18] describes the interaction of fast heavy ions with the inner-shell electrons within the dielectric formalism. It is a high velocity model ($v_p \geqslant v_e$) valid in the small pertubation regime. The LPA assumes that the bound electrons react as free particles to the external perturbation and that they may be described at each point of space as a gas of free electrons with the density given by the initial target state to which they belonged. This approximation is expected to be valid for bound electrons with orbital speed smaller than the ion velocity ($v_p \geqslant v_e$ for *K* shell). However, a very good accord with experimental data is found even for projectile velocities lower than this value [20].

The LPA [17] proposes a dielectric function for the bound electrons, which is a spatial mean value of the Lindhard dielectric function $\varepsilon(q,\omega,n(r))$ [22],

$$\frac{1}{\varepsilon^{\mathrm{LPA}}(q,\omega)} = \frac{3}{R_{WS}^3}\int_0^{R_{WS}} r^2 dr \, \frac{1}{\varepsilon(q,\omega,n(r))}, \qquad (1)$$

with R_{WS} being the Wigner-Seitz sphere radius ($R_{WS} = [3/(4\pi n_{at})]^{1/3}$ and n_{at} the atomic density). In the present calculations, the spatial dependent density $n(r)$ of the shell is obtained from the Hartree-Fock wave functions of the target atoms [23]. The LPA as presented here is specially suitable in the calculation of inner-shell ionization cross sections because we can evaluate each shell separately and take into account the gap (ionization energy) from shell to shell.

The *K*-shell ionization cross section within the LPA model reads as [20]

$$S_K^{\mathrm{LPA}} = \frac{2Z_P^2}{\pi v_p^2 n_{at}} \int_0^\infty \frac{dq}{q} \int_{\epsilon_K}^{q v_p} \mathrm{Im}\left[-\frac{1}{\varepsilon^{\mathrm{LPA}}(q,\omega)} \right] d\omega, \qquad (2)$$

where ϵ_K is the *K*-shell binding energy consistent with the Hartree-Fock wave functions employed in the calculations of $n(r)$ [23]. It is important to note that these ionization cross sections are independent of the atomic density, even when it is included in Eq. (2) and in the LPA the dielectric function as given by Eq. (1). Both contributions cancel each other, and the space integration up to R_{WS} in Eq. (1) converges for radius much lower than R_{WS}, as it is expected for the *K* shell.

III. EXPERIMENTAL DETAILS AND DATA ANALYSIS

A well collimated beam of O ions with energy between 25 and 100 MeV was provided by the BARC-TIFR Pelletron facility at TIFR. The energy and charge state analyzed ion beam was made to pass through a post-acceleration foil stripper to obtain different charge states and a switching magnet was used to select a particular charge state. The targets of Cl, K (in the form of KCl), Ti, Fe, and Cu were prepared on 10 μg/cm^2 thick C backing with thicknesses 1.6, 1.6, 2.43, 0.58, and 1.9 μg/cm^2, respectively. Such thin targets were chosen to ensure single collision conditions [24–26]. The targets were mounted on a rotatable multiple target holder assembly. The x rays were detected using a Si(Li) x-ray detector having 30 mm^2 area and 3 mm thickness. The detector with 25 μm Be window was mounted inside the vacuum chamber at an angle of 45° with respect to the beam direction. The detector had an energy resolution of 165 eV at 5.9 keV. A silicon surface barrier detector was mounted at 135° to detect the elastically scattered particles and was used to measure the target thickness *in situ*. The target chamber was electrically isolated in order to collect the charge on the entire chamber which was used for charge normalization. This was required especially at higher energies, i.e., above Coulomb barrier. The data were collected on a CAMAC based high-speed data-acquisition system interfaced to the PC.

Typical x-ray spectra emitted from the different targets bombarded by 100-MeV oxygen ions are displayed in Fig. 1. In case of Cu, Fe, and Ti, the K_α and K_β lines are well separated whereas for K and Cl, these lines are not well resolved. For the purpose of background subtraction, carbon foils of 10 μg/cm^2 thickness were also mounted. The spectra were analyzed to obtain the peak position and the intensity using a multiparameter fitting program. The intensities were corrected for the detector efficiency and absorption in the Be window. The expression used for calculating the *K*-vacancy cross sections is

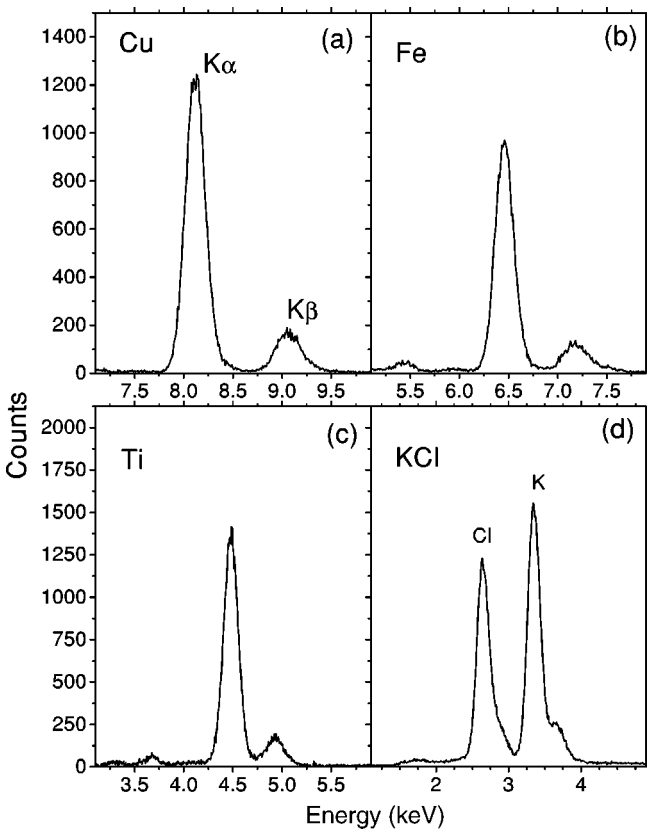

FIG. 1. X-ray spectrum emitted from various targets in collision with 100-MeV O^{7+}.

$$\sigma_{KV}=\frac{4\pi N_x A}{\Delta\Omega_x \epsilon t N_\alpha N_p}\frac{1}{\omega_k}, \tag{3}$$

where N_x is the number of x-ray photons detected. N_p is the number of incident particles, t is the target thickness, ϵ is the efficiency of Si(Li) detector, $\Delta\Omega_x$ is the solid angle covered by x-ray detector, and σ_{KV} being the vacancy production cross section. The fluorescence yields (ω_k) were taken from the tabulation by Krause [27] and the corrections in these values were estimated using data from Bhalla [28–30] and from the measured intensity ratios of K_α and K_β lines and the shifts in the x-ray energies (see Table I). Such corrections in the ω_k values are required due to the multiple ionization in the outer shells. The enhancement was found to be between 9% and 22% (Table I). The *K*-*K* electron transfer cross sections were derived from the measured vacancy production cross sections as a function of the projectile charge state, i.e., as a function of the number of vacancies in the *K* shell of the projectile, such as

$$\sigma_{KK}=\sigma_{KV}^{(1)}-\sigma_{KV}^{(0)} \tag{4}$$

and

$$\sigma_{KK}=\frac{1}{2}(\sigma_{KV}^{(2)}-\sigma_{KV}^{(0)}), \tag{5}$$

where σ_{KK} is the cross section for electron to be transferred from target *K* shell to the projectile *K* shell and σ_{KV}^{i} is the total *K*-vacancy production cross section with "i" number of vacancies in the projectile *K* shell ($i=0,1,2$). The vacancy production cross sections for projectiles with lower charge states, i.e., with no *K*-shell vacancy (σ_{KV}^{0}), are found to be almost independent of charge states and are taken as Coulomb ionization cross sections (σ_{KI}). The derived cross sections are shown in Table I. Typical errors are about 15% for ionization cross sections and about 25% for the transfer data. These errors include the uncertainties in the target thickness, detector solid angles, fluorescence yields, counting statistics, and the procedure to derive the transfer cross sections.

IV. RESULTS AND DISCUSSIONS

A. Ionization

In heavy-ion–atom collisions, the energies of the target K_α and K_β x-ray lines increase from that of a singly ionized atom due to the presence of multiple vacancies in the outer shells. The x-ray energy shifts, as a function of the beam energy, are plotted in Fig. 2 for various target elements. The multiple data points at a given energy correspond to different projectile charge states. It may be seen that the energy shifts do not show any dependence on the charge states unlike that observed in case of gas targets [31]. The reason for the absence of such dependence is that the charge state of the projectile is equilibrated within a few monolayers of the solid target. The uncertainties in the peak energies of K_α and K_β were $\approx$10 eV and 20 eV, respectively. It may be seen that the energy shifts decrease as a function of beam energy (Fig. 2). The beam velocities are between 8 and 14 a.u., which are much larger than the *M*- and *L*-shell orbital velocities of the target electrons, making the *L*- and *M*-shell ionization and transfer cross sections very small. As the beam energy increases, these cross sections fall rapidly resulting in less multiple ionization in *L* and *M* shells.

Figure 3 shows the measured *K*-shell ionization cross sections along with the predictions of the ECPSSR and the LPA models. For the Fe target, the charge state dependence could not be studied and at the two highest energies H-like or bare ions were used in the experiment. Therefore, the vacancy production cross sections at these two energies [shown as squares in Fig. 3(d)] include the *K*-*K* transfer cross sections along with the *K* ionization, $\sigma_{KI}+\sigma_{KK}$.

The ECPSSR model based on ion-atom collisions provides an excellent agreement with the data over the whole range of velocities and for different symmetry parameters [see dotted lines in Figs. 3(a)–3(e)]. For the Fe target, the theoretical calculation shown by dashed line, includes the contributions due to the *K*-*K* transfer process (see below) along with the ECPSSR predictions for *K* ionization. It may be noted that the ECPSSR is a thoroughly developed model, although more semiempirical in nature. A good agreement with the data clearly indicates that for the inner-shell ionization, this ion-atom collision model should be applicable for ion-solid collision experiments provided sufficiently thin targets are used to ensure the single-collision conditions. How-

TABLE I. The σ_{KI}, σ_{KK}, ΔK_α, ΔK_β, and the intensity ratios and the enhancements in fluorescence yields. * denotes σ_{KV} [for H-like ions, see Eq. (3)].

Target	Energy (MeV)	ΔE_α (eV)	ΔE_β (eV)	I_β/I_α	ω_k/ω_o	σ_{KI} (kb)	σ_{KK} (kb)
Cl	25	61	146	0.101	1.22	239	29
	36	56	121	0.121	1.22	473	50
	52	46	86	0.129	1.13	654	89
	64	41	76	0.113	1.13	630	97
	72	41	66	0.128	1.13	618	98
	84	36	56	0.138	1.13	669	54
	100	31	46	0.153	1.05	745	54
K	25	60	162	0.113	1.22	78.6	8.4
	36	55	147	0.131	1.22	183	13.3
	52	45	102	0.161	1.13	315	18.5
	64	40	82	0.156	1.13	356	55
	72	41	61	0.168	1.13	367	25.2
	84	36	62	0.172	1.13	408	23.7
	100	30	47	0.176	1.05	480	22
Ti	25	61	167	0.163	1.29	16.4	0.2
	36	61	157	0.153	1.29	55.8	3.1
	52	51	121	0.131	1.21	121	4.8
	64	45	101	0.136	1.15	171	20.6
	72	40	91	0.138	1.13	203	
	84	35	76	0.128	1.12	173	20
	100	30	81	0.137	1.12	195	
Fe	40	60	165	0.162		16.92	
	54	55	152	0.172		36.7	
	70	55	102	0.165		52.36	
	85	50	91	0.171		72.5*	
	100	50	78	0.157		116*	
Cu	25	55	145	0.168	1.08	0.7	0.12
	36	60	145	0.181	1.14	2.53	0.6
	40	60	160	0.188	1.14	6.19	
	52	50	140	0.174	1.13	9.03	2.05
	54	60	140	0.177	1.13	14.1	
	64	50	125	0.165	1.13	15.7	4.2
	70	50	130	0.171	1.13	21	
	72	45	120	0.164	1.11	22	3.7
	84	40	115	0.161	1.11	32.8	2.3
	85	50	120	0.1595	1.11	38	
	100	35	95	0.157	1.09	31.2	7.85

ever, the applicability of the ECPSSR depends very much on the collision symmetry parameter. For example, Dhal *et al.* [32] has shown that the model deviates from the measured data for more symmetric collision system (such as Si on Ar) for which S_Z was 0.78.

On the other hand, the LPA behavior is acceptable, but tends to underestimate the data for the most symmetric collisions. As can be seen from Fig. 3, the LPA agrees well with the data in case of Cu at higher velocities and deviates in the lower-energy region. Similarly in case of Fe, the LPA reproduces the data quite well (except for the highest two energies for which the measured data include $\sigma_{KI}+\sigma_{KK}$, whereas the

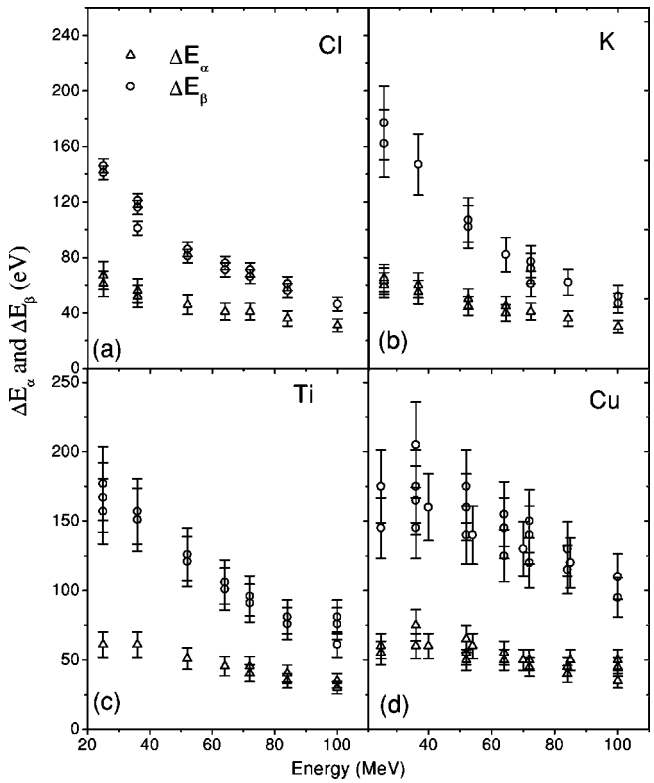

FIG. 2. Energy shifts of the K_α and K_β lines for Cl (a), K (b), Ti (c), and Cu (d) targets in collisions with oxygen ions. The different data points (i.e., same symbol) at the same energy correspond to different charge states of the projectile.

present LPA gives ionization cross sections). The agreement is even reasonable for Ti target except for the lowest energy. For the low Z targets (i.e., for Cl and K), the LPA starts deviating from the data and the deviation is greater on the higher-energy side, which is not expected since this model is supposed to work better at higher energies. A maximum deviation of about 20–45 % is to be noticed for the lowest-Z target used (i.e., for Cl) for which the $S_Z=0.47$. It may thus be concluded that for K ionization, the LPA works better for more asymmetric collision partners such that $S_Z \leqslant 0.35$ above which it starts deviating (at least in the intermediate velocity range).

The deviation in the LPA curves at the lowest velocities considered is expected because in these cases, impact velocities are much lower than the electron velocity in the K shell. In these cases, the free-electron-gas approximation is supposed to fail. This low-energy limit is again related to S_Z. This relation between symmetry and impact velocities can be expressed in terms of the generalized perturbation strength $S_p=Z_p/(v_p Z_t)$, proposed by Tiwari *et al.* [33]. We can summarize the LPA results shown in Fig. 3 by saying that the LPA description is good for $S_p \leqslant 0.03$.

However, it is observed that the *ab initio* model LPA provides quite a good qualitative agreement with the experiment. There is still a scope to improve the LPA model in order to explain the data in the intermediate energy range. The employment of the LPA to describe the K-shell electron response to the ion perturbation, means exploring the limits

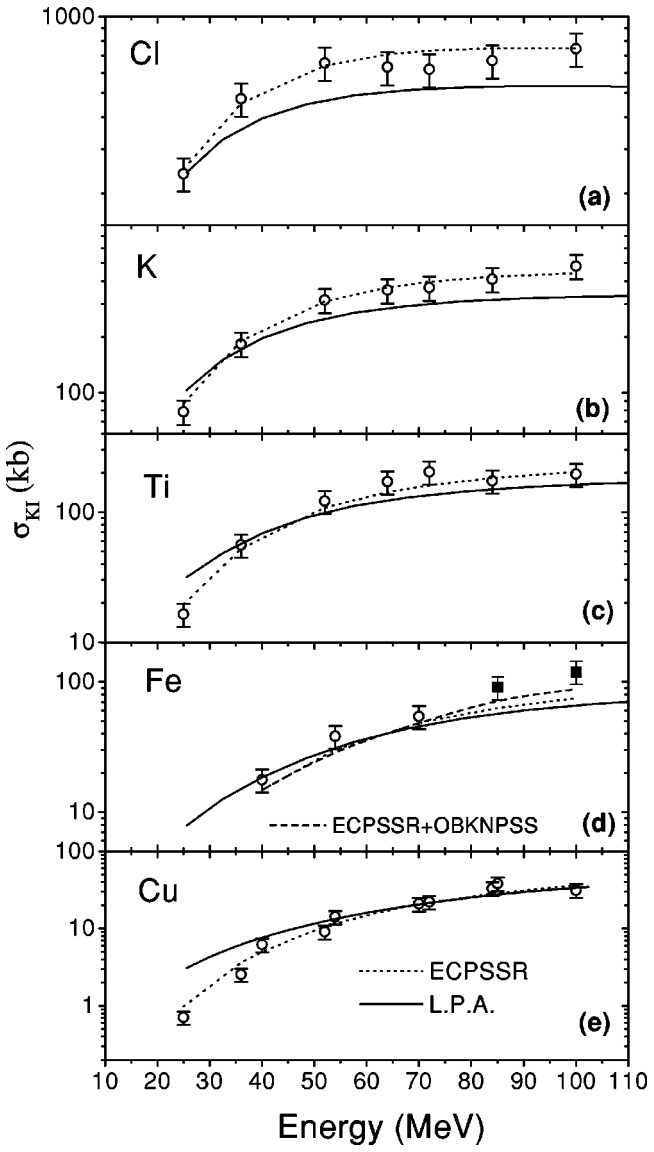

FIG. 3. The *K*-shell ionization cross sections for different targets as a function of beam energy. The charge states of the oxygen ions correspond to zero vacancy in the *K* shell. The LPA and ECPSSR calculations are shown as solid and dotted lines, respectively. In (d) the data at two highest energies correspond to O^{7+} and include the contributions from ionization and *K*-*K* transfer and therefore are to be compared with ECPSSR + OBKNPSS (dashed line).

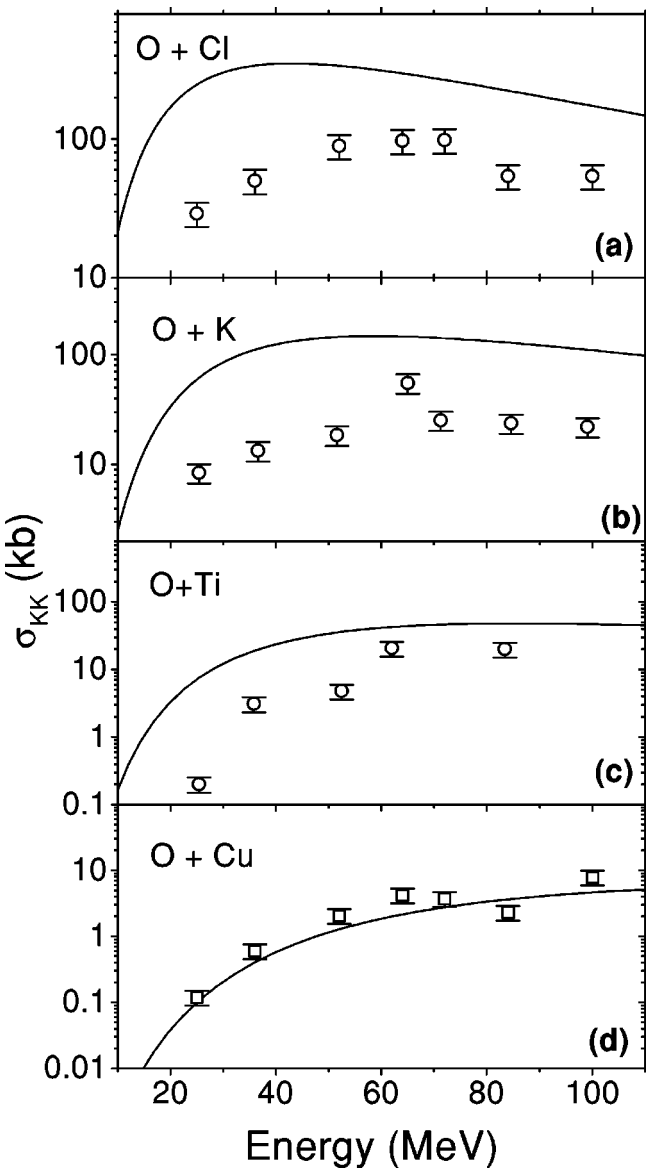

FIG. 4. The measured *K*-*K* electron transfer cross sections for Cl (a), K (b), Ti (c), and Cu (d) targets along with the OBKNPSS calculations (solid lines).

of the model under the worst conditions. The free-electron-gas description of a few highly bound electrons (i.e., the *K* shell) is expected to be worse than that for more weakly bound electrons such as those in the *L* or *M* shells.

B. Electron transfer

The *K*-*K* and *L*-*K* electron transfer cross sections have been measured in a few cases in the past [25,26,31,32,34–36]. Figure 4 shows the present measurements of the *K*-*K* transfer cross sections, derived from the charge state dependence of the x-ray yields as discussed before. The data for Cl, K, Ti, and Cu targets are shown in Figs. 4(a)–4(d). It is well known that the first-order calculation based on the OBKN (Oppenheimer-Brinkman-Kramer-Nikoleav) approximation [37] overestimates the cross sections of inner-shell electron transfer by a large factor. In perturbed-stationary-state approach, Lapicki and McDaniel (1980) [38] have included the second Born term and the corrections due to the enhanced binding energy and Coulomb deflection in the OBKN formalism, in the same way as was done in the ECPSSR formalism for ionization. Although this formalism is not an *ab initio* one, the simplicity of using analytical expression in this method and its ability to predict the cross sections for asymmetric collisions is worth mentioning. Comparison of this model (OBKNPSS) with the experimental data for different symmetry parameters is displayed in Fig. 4. The best agreement is found for the most asymmetric collision partners, i.e., for O+Cu, for which the calculation reproduces the data very well over the entire energy range.

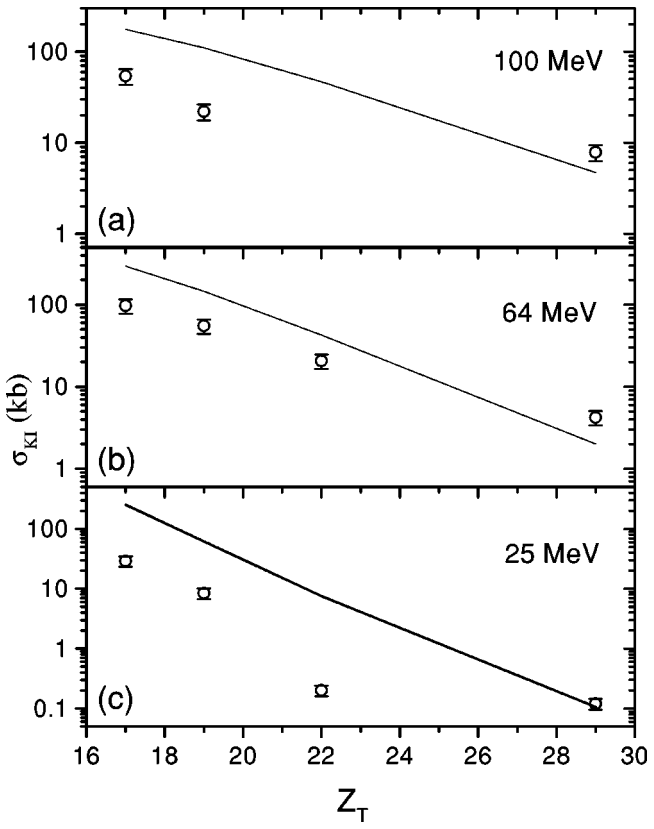

FIG. 5. Variation of *K*-*K* electron transfer cross sections as a function of target atomic number Z_t for three different energies, as indicated. The solid lines are the OBKNPSS calculations.

The model deviates from the data substantially with increasing S_Z, i.e., for Ti, K, and Cl targets. In the case of the most symmetric system studied, i.e., O+Cl, the deviation is the largest amounting to a factor of about 8 at low energies. This factor is reduced to about 3 at higher energies. The perturbation strength being very large for these collision systems, the PSS approach fails even for the relatively asymmetric collision partners, i.e., for $S_Z \geqslant 0.3$.

In Fig. 5, we display the σ_{KK} as a function of Z_t. The data are shown for three different beam energies, i.e., 100 MeV [Fig. 5(a)], 64 MeV [Fig. 5(b)], and 25 MeV [Fig. 5(c)]. The best agreement is always found at the highest Z_t studied here (i.e., for Cu) at all three energies shown. With higher Z_t the electron is more strongly bound, making the perturbation strength small and therefore making the PSS approach applicable. However, the close-coupling calculations [39] have been shown to give a better agreement for such state selective capture processes, especially for the near symmetric collision systems [31,25,32]. These calculations are not available for the present collisions.

Following the suggestion made by Tiwari *et al.* [33], we can discuss the comparison with the OBKNPSS behavior in terms of the generalized perturbation strength, defined before. Physically, S_p is small for large collision velocity and for the tightly bound electrons, i.e., for large Z_t. This aspect is explained in Fig. 6, in which we show the ratio of the data to the OBKNPSS calculations as a function of S_p. It is clearly seen that the ratio is close to 1.0 only for the lowest

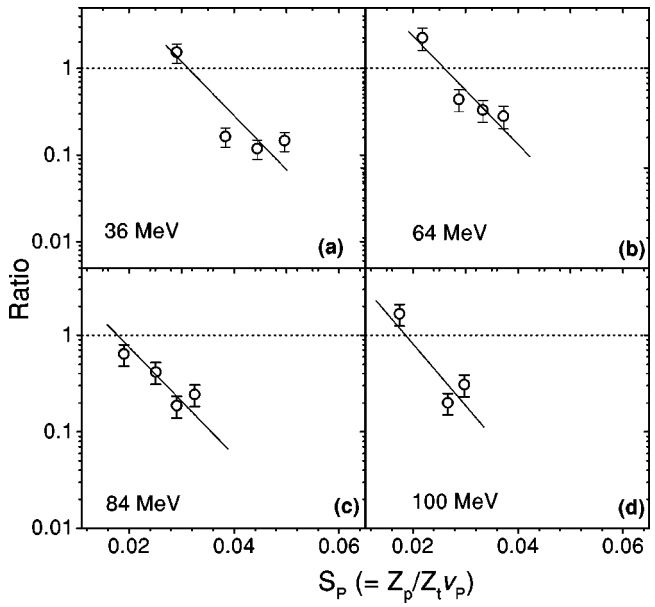

FIG. 6. The ratio of measured σ_{KK} to the OBKNPSS calculations vs the perturbation strength (see text). The straight lines through the data points are to guide the eyes.

perturbation strength, i.e., for $S_p = 0.017$ (at 100 MeV) to 0.029 (at 36 MeV), and deviates largely for higher values of S_p. As the S_p increases, the ratio decreases rapidly, in all four energies shown in Figs. 6(a–d). The straight lines through the ratio are to guide the eyes and may provide quantitative information on the degree of deviation of the theory as a function of the generalized perturbation strength.

It must be mentioned that for the *K*-*K* transfer process, we do not have a collective response theory coming from the dielectric formalism in order to compare binary and collective models applied to ion-solid collisions. It remains to be investigated whether it is possible to have such a LPA model to describe state selective electron transfer processes in ion-solid collisions.

V. CONCLUSIONS

K-shell vacancy production cross sections arising from Coulomb ionization and state selective *K*-*K* electron transfer processes are measured in collisions of oxygen ions with solid targets of low atomic numbers ($17 \leqslant Z_t \leqslant 29$) in the intermediate velocity range. The investigation was extended over a wide range of collision symmetry parameter (S_Z between 0.27 and 0.47) and the generalized perturbation strength (S_p between 0.017 and 0.06). The measured ionization cross sections were used to provide a test to the local plasma approximation, which has been developed from the dielectric formalism to include the solid-state effect on atomic collisions. The *ab initio* LPA model, although, is found to give an overall acceptable agreement but tends to underestimate the data for symmetric collisions and low velocities. The LPA description of the *K*-shell ionization is good for $S_p \geqslant 0.03$. On the other hand, the ECPSSR model, which is throughly developed but more semiempirical in nature, shows an excellent agreement with the measurements

even for the low Z_t targets in the whole energy range considered here. The measured *K*-*K* electron transfer cross sections are found to be reproduced by the PSS calculations only for highly asymmetric collision partners such as O + Cu. Again the comparison with models are presented in terms of the generalized perturbation strength. The need of a model that describes state selective electron transfer process, proceeding from the dielectric formalism so as to incorporate solid-state effects, is emphasized. It is shown that the model should be improved to explain the collision aspects in the intermediate energy range. The limitation of the free-electron-gas approximation applied to describe the *K*-shell ionization has been pointed out.

ACKNOWLEDGMENTS

The authors thank the Pelletron accelerator staff for the smooth operation of the machine and K.V. Thulasiram for his assistance during the experiment. They also thank J. E. Miraglia for fruitful discussions and comments on the theoretical description.

[1] W. Brandt and G. Lapicki, Phys. Rev. A **23**, 1717 (1981), and references therein.
[2] G. Lapicki, J. Phys. Chem. Ref. Data **18**, 111 (1989).
[3] A.S. Schlachter, J.W. Stearns, W.G. Graham, K.H. Berkner, R.V. Pyle, and J.A. Tanis, Phys. Rev. A **27**, 3372 (1983).
[4] H. Knudsen, H.K. Haugen, and P. Hvelplund, Phys. Rev. A **23**, 597 (1981).
[5] G. Basbas, W. Brandt, and R. Laubert, Phys. Rev. A **7**, 983 (1973).
[6] G. Basbas, W. Brandt, and R. Laubert, Phys. Rev. A **17**, 1655 (1978).
[7] N. Bohr, K. Dan. Vidensk. Selsk. Mat. Fys. Medd. **18**, 8 (1948).
[8] P.M. Echenique, F. Flores, and R.H. Ritchie, Solid State Phys. **43**, 229 (1990), and references therein.
[9] J. Burgdoerfer, Nucl. Instrum. Methods Phys. Res. B **67**, 1 (1992), and refernces therein.
[10] L.C. Tribedi, V. Nanal, M.R. Press, M.B. Kurup, K.G. Prasad, and P.N. Tandon, Phys. Rev. A **49**, 374 (1994).
[11] L.C. Tribedi, V. Nanal, M.B. Kurup, K.G. Prasad, and P.N. Tandon, Phys. Rev. A **51**, 1312 (1995).
[12] J.P. Rozet, A. Chetioui, P. Bouisset, D. Vernhet, K. Wohrer, A. Touati, C. Stephan, and J.P. Grandin, Phys. Rev. Lett. **58**, 337 (1987).
[13] U. Kadhane, D. Misra, Y.P. Singh, and Lokesh C. Tribedi, Phys. Rev. Lett. (to be published).
[14] U. Kadhane, Y.P. Singh, D. Misra, and Lokesh C. Tribedi, Nucl. Instrum Methods Phys. Res. B (to be published).
[15] J-P. Rozet, D. Vernhet, I. Bailly-Despiney, C. Fourment, and L.J. Dubé, J. Phys. B **32**, 4677 (1999).
[16] D. Vernhet, J-P. Rozet, I. Bailly-Despiney, C. Stephan, A. Casssimi, J-P. Gradin, and L.J. Dubé, J. Phys. B **31**, 117 (1998).
[17] J.D. Fuhr, V.H. Ponce, F.J. Garcia de Abajo, and P.M. Echenique, Phys. Rev. B **57**, 9329 (1998).
[18] J. Lindhard and M. Scharff, K. Dan. Vidensk. Selsk. Mat. Fys. Medd. **27**, 15 (1953).
[19] A. Sarasola, J.D. Fuhr, V.H. Ponce, and A. Arnau, Nucl. Instrum. Methods Phys. Res. B **182**, 67 (2001).
[20] C.C. Montanari, J.E. Miraglia, and N.R. Arista, Phys. Rev. A **66**, 042902 (2002).
[21] J. Calera-Rubio, A. Gras-Marti, and N.R. Arista, Nucl. Instrum. Methods Phys. Res. B **93**, 137 (1994).
[22] J. Lindhard, K. Dan. Vidensk. Selsk. Mat. Fys. Medd. **28**, 8 (1954).
[23] E. Clementi and C. Roetti, At. Data Nucl. Data Tables **14**, 177 (1974).
[24] T.J. Gray, in *Methods of Experimental Physics*, edited by P. Richard (Academic, New York, 1980), Vol. 17, p. 193.
[25] J. Hall *et al.*, Phys. Rev. A **33**, 914 (1986).
[26] L.C. Tribedi, K.G. Prasad, P.N. Tandon, Z. Chen, and C.D. Lin, Phys. Rev. A **49**, 1015 (1994); L.C. Tribedi, K.G. Prasad, and P.N. Tandon, *ibid.* **47**, 3739 (1993).
[27] M.O. Krause, J. Phys. Chem. Ref. Data **8**, 307 (1979).
[28] C.P. Bhalla, Phys. Rev. A **8**, 2877 (1973).
[29] C.P. Bhalla, Phys. Rev. A **12**, 122 (1975).
[30] C.P. Bhalla, J. Phys. B **8**, 1200 (1975).
[31] B.B. Dhal, L.C. Tribedi, U. Tiwari, K.V. Thulasiram, P.N. Tandon, T.G. Lee, C.D. Lin, and L. Gulyas, Phys. Rev. A **62**, 022714 (2000).
[32] B.B. Dhal, L.C. Tribedi, U. Tiwari, P.N. Tandon, Teck Lee, and C.D. Lin, J. Phys. B **33**, 1096 (2000).
[33] U. Tiwari, A.K. Saha, L.C. Tribedi, M.B. Kurup, P.N. Tandon, and L. Gulyaś, Phys. Rev. A **58**, 4494 (1998).
[34] K. Wohrer, Chetioui, J.P. Rozet, A. Jolly, and C. Stephan, J. Phys. B **17**, 1575 (1984).
[35] J.A. Tanis, S.M. Shafroth, J.E. Willis, J.R. Mowat, Phys. Rev. Lett. **45**, 1547 (1980).
[36] B.B. Dhal, A.K. Saha, Lokesh C. Tribedi, K.G. Prasad, and P.N. Tandon, J. Phys. B **31**, L807 (1998).
[37] V.S. Nikolaev, Sov. Phys. JETP **24**, 847 (1967), and references therein.
[38] G. Lapicki and F.D. McDaniel, Phys. Rev. A **22**, 1896 (1980).
[39] W. Fritsch and C.D. Lin, Phys. Rep. **202**, 1 (1991).